ORGANOMETALLICS

Synthesis and characterization of (CP)2Mo2(CO)4(.mu.-.eta.2:.eta.2-FP-C.tplbond.C-H), adducts of ethynyliron complexes to (CP)2Mo2(CO)4: their fluxional behavior via reversible 1-alkyne-vinylidene ligand interconversion on a dinuclear system and photochemical decarbonylation leading to the .mu.3-vinylidenyl complexes (CP)FeCp2Mo2(CO)4(.mu.-CO)(.mu.3-:C:CH)

Munetaka Akita, Shuichiro Sugimoto, Akio Takabuchi, Masako Tanaka, and Yoshihiko Morooka

Organometallics, **1993**, 12 (8), 2925-2932• DOI: 10.1021/om00032a013 • Publication Date (Web): 01 May 2002

Organometallics **1993,** *12,* 2925–2932

Synthesis and Characterization of $(CP)_2Mo_2(CO)_4(\mu\text{-}\eta^2{:}\eta^2\text{-}FP{-}C{\equiv}C{-}H)$, Adducts of Ethynyliron Complexes to $(CP)_2Mo_2(CO)_4$: Their Fluxional Behavior via Reversible 1-Alkyne–Vinylidene Ligand Interconversion on a Dinuclear System and Photochemical Decarbonylation Leading to the μ_3-Vinylidenyl Complexes $(CP)FeCp_2Mo_2(CO)_4(\mu\text{-}CO)(\mu_3\text{-}{=}C{=}CH)$[†]

Munetaka Akita,* Shuichiro Sugimoto, Akio Takabuchi, Masako Tanaka, and
Yoshihiko Moro-oka*

Research Laboratory of Resources Utilization, Tokyo Institute of Technology, 4259 Nagatsuta, Midori-ku, Yokohama 227, Japan

Received March 2, 1993

Interaction of the ethynyliron complexes FP—C≡C—H (**1**) with $(CP)_2Mo_2(CO)_4$ (**2**) affords the adducts $(CP)_2Mo_2(CO)_4(\mu\text{-}\eta^2{:}\eta^2\text{-}FP{-}C{\equiv}C{-}H)$ (**3**) with the tetrahedral C_2Mo_2 core in a manner similar to the reaction of alkynes. Although the molecular structures of $Cp_2Mo_2(CO)_4(\mu\text{-}\eta^2{:}\eta^2\text{-}Fp{-}C{\equiv}C{-}H)$ (**3a**) and $Cp_2Mo_2(CO)_4(\mu\text{-}\eta^2{:}\eta^2\text{-}Fp^{Si}{-}C{\equiv}C{-}H)$ (**3e**) are close to those of normal alkyne adducts with the exception of the Mo–C(Fe) distances being slightly longer than the Mo–C(H) distances, **3** shows complicated dynamic behavior. Variable-temperature ^{13}C NMR analyses of **3** have revealed two characteristic features: (1) The two sharp C_2H doublets observed at low temperature broaden in the medium-temperature range and finally appear as two signals at the fast-exchange limit. This behavior is interpreted in terms of a reversible 1,2-H migration mechanism via the vinylidene intermediate $(CP)_2Mo_2(CO)_4[\mu\text{-}\eta^1{:}\eta^2\text{-}C{=}C(H)FP]$ (**C**). (2) All the Mo–CO's are observed equivalently at higher temperature via an undetermined process. Irradiation of **3a**,**b** results in decarbonylation to give the isomeric mixture of μ_3-vinylidenyl complexes $(CP)FeCp_2Mo_2(CO)_4(\mu\text{-}CO)(\mu_3\text{-}C_2H)$ with an Mo–Mo–Fe linkage (**5a**, CP = Cp; **5b**, CP = Cp*). The structure of **5a** determined crystallographically is described as the dimolybdenum $\mu\text{-}\eta^1{:}\eta^2$-vinylidene complex $Mo_2(\mu\text{-}\eta^1{:}\eta^2\text{-}{=}C{=}CR_2)$ bearing an Fe group as one of the vinylidene substituents (R). The formation and the structure of **5a** support **C**. Crystal data: **3a**, $C_{23}H_{16}O_6FeMo_2$, space group $P2_1/a$ (monoclinic), $a = 18.318(2)$ Å, $b = 9.709(2)$ Å, $c = 12.608(3)$ Å, $\beta = 98.85(1)°$, $V = 2216(1)$ Å^3, $Z = 4$, R (R_w) = 0.044 (0.039); **3e**, $C_{26}H_{24}O_6SiFeMo_2$, space group $P2_1/c$ (monoclinic), $a = 12.608(2)$ Å, $b = 23.224(12)$ Å, $c = 9.172(2)$ Å, $\beta = 96.11(2)°$, $V = 2670(3)$ Å^3, $Z = 4$, R (R_w) = 0.051 (0.056); **5a**, $C_{22}H_{16}O_5FeMo_2$, space group $P2_1/a$ (monoclinic), $a = 15.197(3)$ Å, $b = 17.362(5)$ Å, $c = 8.080(3)$ Å, $\beta = 101.32(2)°$, $V = 2090(1)$ Å^3, $Z = 4$, R (R_w) = 0.046 (0.039).

Introduction

We have been studying polymetallic C_2H_n complexes (n = 0, 1) derived from parent iron acetylides, i.e. the ethynyliron complexes FP—C≡C—H and the ethynediyldiiron complex Fp*—C≡C—Fp*.[1-4] Such hydrogen-poor hydrocarbyl species (C_2H_n) may form at an early stage of heterogeneous reactions such as catalytic CO hydrogenation.[6] This study stems from our expectation that, with respect to the coordination structure and chemical properties, the C_2H_n ligands of simple composition should be closer to the actual surface-bound hydrocarbyl species compared to those derived from acetylides with an organic substituent such as alkyl, Ph, and CO_2R.[5]

The parent iron acetylides readily react with a variety of mono-,[1a] di-,[1c,d] and trimetallic species[1e] to give poly-

---

[†] Abbreviations used in this paper: FP = $CPFe(CO)_2$ (Fp = $CpFe(CO)_2$, Fp* = $Cp^*Fe(CO)_2$, Fp′ = $Cp'Fe(CO)_2$, Fp^{Si} = $Cp^{Si}Fe(CO)_2$); CP = $\eta^5\text{-}C_5R_5$ (Cp = $\eta^5\text{-}C_5H_5$, Cp* = $\eta^5\text{-}C_5Me_5$, Cp′ = $\eta^5\text{-}C_5H_4Me$, Cp^{Si} = $\eta^5\text{-}C_5H_4SiMe_3$).

(1) (a) Akita, M.; Oyama, S.; Terada, M.; Moro-oka, Y. *Organometallics* **1990**, *9*, 816–825. (b) Akita, M.; Oyama, S.; Terada, M.; Moro-oka, Y. *Organometallics* **1991**, *10*, 1561–1568. (c) Akita, M.; Terada, M.; Moro-oka, Y. *Organometallics* **1991**, *10*, 2961–2965. (d) Akita, M.; Terada, M.; Moro-oka, Y. *Organometallics* **1992**, *11*, 1825–1830. (e) Akita, M.; Terada, M.; Moro-oka, Y. *Organometallics* **1992**, *11*, 3468–3472. (f) Akita, M.; Sugimoto, S.; Tanaka, M.; Moro-oka, Y. *J. Am. Chem. Soc.* **1992**, *114*, 7581–7582.

(2) Ethynyl complexes (M—C≡C—H). (a) M = Fp*: Reference 1a. (b) M = Fp: Kim, P. J.; Masai, H.; Sonogashira, K.; Hagihara, N. *Inorg. Nucl. Chem. Lett.* **1970**, *6*, 181–185. (c) M = CpFe(dppe): Davison, A.; Selegue, J. P. *J. Am. Chem. Soc.* **1978**, *100*, 7763–7765. (d) M = $CpFe(CO)(PPh_3)$: Boland-Lussier, B. E.; Churchill, M. R.; Hughes, R. P.; Rheingold, A. L. *Organometallics* **1982**, *1*, 628–634. (e) M = CpFe(dppm): Gamasa, M. P.; Gimeno, J.; Lastra, E.; Lanfranchi, M.; Tiripicchio, A. *J. Organomet. Chem.* **1991**, *405*, 333–345. (f) M = group 11 metal: Nast, R. *Coord. Chem. Rev.* **1982**, *47*, 89–124. (g) M = $CpNi(PPh_3)$: Yamazaki, H.; Nishido, Y.; Matsumoto, Y.; Sumida, S.; Hagihara, N. *J. Organomet. Chem.* **1966**, *6*, 86–91. (h) M = $CpNi(PPh_3)$, $Pd(PR_3)_2X$, $Pt(PR_3)_2X$: Sonogashira, K.; Fujikura, Y.; Yatake, T.; Tohda, Y.; Takahashi, S.; Hagihara, N. *J. Chem. Soc., Chem. Commun.* **1977**, 291–292. (i) M = $Pt(PR_3)_2X$: Sonogashira, K.; Fujikura, Y.; Yatake, T.; Toyoshima, N.; Takahashi, S.; Hagihara, N. *J. Organomet. Chem.* **1978**, *145*, 101–108. (j) M = $Pt(PR_3)_2X$: Bell, R. A.; Chisholm, M.; Cough, D. A.; Rankel, L. A. *Inorg. Chem.* **1977**, *16*, 677–686. (k) M = $Re(CO)_5$: Appel, M.; Heidrich, J.; Beck, W. *Chem. Ber.* **1987**, *120*, 1087–1089. (l) M = $Rh^+[N(CH_2CH_2PPh_2)_3](H)$, $Rh^+[P(CH_2CH_2PPh_2)_3](H)$: Bianchini, C.; Masi, D.; Meli, A.; Peruzzini, M.; Ramirez, J. A. *Organometallics* **1989**, *8*, 2179–2189.

0276-7333/93/2312-2925$04.00/0

metallic adducts. As an extension, we examined interaction with the coordinatively unsaturated dimolybdenum species $Cp_2Mo_2(CO)_4$. It has been well established that alkynes add across the metal–metal triple bond in $Cp_2Mo_2(CO)_4$ to give the adducts $Cp_2Mo_2(CO)_4(\mu\text{-}\eta^2{:}\eta^2\text{-}R\text{-}C{\equiv}C\text{-}R)$ (**A**) with a tetrahedral C_2Mo_2 core (eq 1).[8] Most

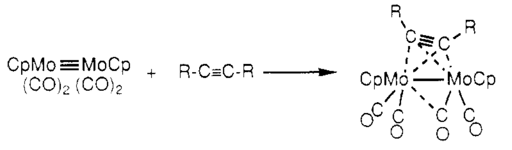

(1)

A

of the resulting adducts, owing to the occurrence of the semibridging CO ligand, possess no symmetry in the solid state and even in solution at low temperature.[9] However, at higher temperature the fast switching process of the CO ligands allows the adducts to adopt a time-averaged higher symmetry, i.e. C_s and C_{2v} symmetry for unsymmetrically and symmetrically-substituted alkyne adducts, respectively. Herein we report the preparation and structure determination of the adducts derived from the ethynyliron complexes as well as their fluxional behavior via an H migration. Photochemical decarbonylation of the adducts leading to μ_3-vinylidenyl complexes is also disclosed.

Results and Discussion

Preparation and Characterization of $(CP)_2Mo_2(CO)_4(\mu\text{-}\eta^2{:}\eta^2\text{-}FP{-}C{\equiv}C{-}H)$(3). Reaction of the ethynyliron complexes FP—C≡C—H (**1**; FP = Fp (**a**), Fp* (**b**), Fp′ (**c**), Fp^{Si} (**d**)) with isolated or *in situ* generated $(CP)_2Mo_2(CO)_4$ (**2**; CP = Cp (**a**), Cp′ (**b**))[7] at room temperature readily afforded the adducts $(CP)_2Mo_2(CO)_4(\mu\text{-}\eta^2{:}\eta^2\text{-}FP{-}C{\equiv}C{-}H)$ (**3**; FP, CP = Fp, Cp (**a**), Fp*, Cp (**b**), Fp*, Cp′ (**c**), Fp′, Cp (**d**), Fp^{Si}, Cp (**e**)) in good yields after simple crystallization (eq 2).[8] However, the reaction

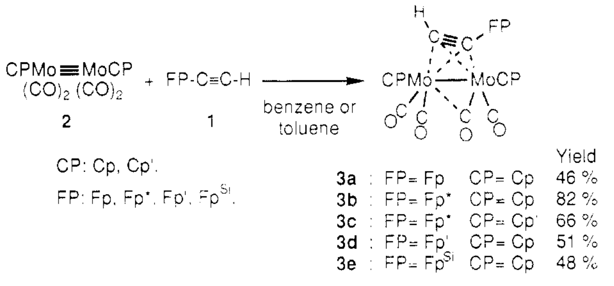

(2)

of **1a** with the tungsten analogue $[Cp_2W_2(CO)_4]$ and the reaction of the ethynediyl complex Fp*—C≡C—Fp* with **2a** resulted in simple CO transfer to give $Cp_2M_2(CO)_6$ after a prolonged reaction period.

The following spectroscopic analyses of **3a** indicate the formation of the expected complexes. The ^1H NMR spectra are consistent with the compositions, and the $C_2\mathit{H}$ signals (δ 6.76–7.06) appear in slightly lower field than those of the normal 1-alkyne adducts $Cp_2Mo_2(CO)_4(\mu\text{-}R{-}C{\equiv}C{-}H)$ $\delta(C_2\mathit{H})$ (R): 4.97 (H, **4a**), 5.35 (Ph, **4b**), 5.43 (CF_3), 5.97 (CH_2CH_2OH)).[8b,9] The IR spectra with low-frequency absorptions suggest the presence of the semibridging CO ligand. However, the ^{13}C NMR spectrum of **3a** recorded at 27 °C, where the C_2H signals cannot be located and only four signals assignable to CpFe, CpMo, Fe–CO, and Mo–CO are observed, suggests the occurrence of some fluxional behavior (Table I). When the temperature is lowered below −60 °C, the expected spectrum containing the two doublets of the C_2H part (δ 60.8 (J = 10.8 Hz, C_α), 110.0 (J = 212.6 Hz, C_β)) and six CO signals is obtained. (The carbon atoms in **3** are denoted as follows: Fe—C_α≡C_β—H.) The δ_C values of the $CpMo(CO)_2$ parts are comparable to those of **4a**,**b** (Table I).[9] The fluxional behavior will be discussed in the next part.

The molecular structures of **3a**,**e** have been confirmed by X-ray crystallography (Figures 1 and 2). The crystal data are listed in Table II, and selected structural parameters are compared with those of related compounds in Table III. The acetylenic part of **1a**,**d** coordinates perpendicularly to the dimolybdenum center to form the dimetallatetrahedrane core, whose structural parameters are essentially the same as those of the ethyne adduct **4a** (Table III).[9] The C≡C distance elongates by ca. 0.15 Å compared to that in **1b** (1.173(4) Å).[1a] It is notable that the C1–Mo bonds are slightly longer than the C2–Mo bonds by 0.12–0.16 Å as observed for other **1a** adducts with a tetrahedral C_2M_2 core ($Co_2(CO)_6(\mu\text{-}\eta^2{:}\eta^2\text{-}Fp{-}C{\equiv}C{-}H)$ (ca. 0.10 Å)[1d] and $Cp_2Ni_2(\mu\text{-}\eta^2{:}\eta^2\text{-}Fp{-}C{\equiv}C{-}H)$[1e] (ca. 0.09 Å)). However, this distortion may not be due to the vinylidene resonance structure **B** (Chart I), which accounts for the situation of the Co_2 and Ni_2 adducts ($\delta_C(C_\alpha)$ (102.2 (Co), 127.5 (Ni)) > $\delta_C(C_\beta)$ (95.7 (Co), 100.5 (Ni)). In contrast to these adducts, the fact that C_α of **3a** (δ_C 60.8) resonates at considerably higher field than C_β (δ_C 110.0) does is not compatible with **B**[10] and presumably results

---

(3) Ethynediyldimetal complexes (M—C≡C—M). (a) M = Fp*: Reference 1a. (b) M = $CpRu(CO)_2$: Koutsantonis, G.; Selegue, J. P. *J. Am. Chem. Soc.* **1991**, *113*, 2316–2317. (c) M = Ru–W, Fe–W: Frank, K. G.; Selegue, J. P. *J. Am. Chem. Soc.* **1990**, *112*, 6414–6416. (d) M = $Pd(PR_3)_2X$, $Pt(PR_3)_2X$: Ogawa, H.; Onitsuka, K.; Joh, T.; Takahashi, K.; Yamazaki, H. *Organometallics* **1988**, *7*, 2257–2260. (e) M = $Re(CO)_5$: See ref 2k. (f) Heidrich, J.; Steimann, M.; Appel, M.; Beck, W.; Phillips, J. R.; Trogler, W. C. *Organometallics* **1990**, *9*, 1296–1300. (g) M = $CpW(CO)_3$: Chan, M.-C.; Tsai, Y.-J.; Chen, C.-T.; Lin, Y.-C.; Tseng, T.-W.; Lee, G.-H.; Wang, Y. *Organometallics* **1991**, *10*, 378–380. (h) M = Cp^*_2Sc: St. Clair, M.; Schaefer, W. P.; Bercaw, J. E. *Organometallics* **1991**, *10*, 525–527. (i) M = $Mn(CO)_5$: Davis, J. A.; El-Ghanam, M.; Pinckerton, A. A.; Smith, D. A. *J. Organomet. Chem.* **1991**, *409*, 367–376. (j) See also references cited in ref 3b. (k) M = Ru, Zr: Lemke, F. R.; Szalda, D. J.; Bullock, M. *J. Am. Chem. Soc.* **1991**, *113*, 8466–8477. (l) M = Re, Pt: Ramsden, J. A.; Weng, W.; Arif, A. M.; Gladysz, J. A. *J. Am. Chem. Soc.* **1992**, *114*, 5890–5891.

(4) $(\mu_n\text{-}C_2)M_n$ complexes. n = 2: (a) Neithamer, D. R. LaPointe, R. E.; Wheeler, R. E.; Richeson, D. S.; Van Duyne, G. D.; Wolczanski, P. T. *J. Am. Chem. Soc.* **1989**, *111*, 9056–9072. (b) Listemann, M. L.; Schrock, R. R. *Organometallics* **1985**, *4*, 74–83. (c) Caulton, K. G.; Cayton, R. H.; Chisholm, M. H.; Huffman, J. C.; Lobkovsky, E. B.; Xue, *Z. Organometallics* **1992**, *11*, 321–326. n = 3: (d) Blau, R. J.; Chisholm, M. H.; Folting, K.; Wang, R. J. *J. Am. Chem. Soc.* **1987**, *109*, 4552–4560. (e) Weidmann, T.; Weinrich, V.; Wagner, B.; Robl, C.; Beck, W. *Chem. Ber.* **1991**, *124*, 1363–1368. n = 4: (f) Bruce, M. I. *J. Organomet. Chem.* **1990**, 394, 365–384. (g) Jensen, M. P.; Sabat, M.; Shriver, D. F. *J. Cluster Sci.* **1990**, *1*, 75–91. (h) See refs 1d,e and 4j. n = 5: (i) Adams, C. J.; Bruce, M. I.; Skelton, B. W.; White, A. H. *J. Organomet. Chem.* **1992**, 423, 97–104. (j) Adams, C. J.; Bruce, M. I.; Skelton, B. W.; White, A. H. *J. Chem. Soc., Chem. Commun.* **1992**, 26–29. n = 6: (k) Penfold, B. R.; Robinson, B. H. *Acc. Chem. Res.* **1973**, *6*, 73–80. (l) Jensen, M. P.; Phillips, D. A.; Shriver, D. F. *Organometallics* **1992**, *11*, 1859–1869. (m) Gervasio, G.; Rossetti, R.; Stanghellini, P. L.; Bor, G. *Inorg. Chem.* **1984**, *23*, 2073–2079. n = 8: (n) Reference 1f. Encapsulated cluster: (o) Halet, J.-F.; Mingos, D. M. P. *Organometallics* **1988**, *7*, 51–58 and references cited therein. (p) Hayward, C.-M. T.; Shapley, J. R.; Churchill, M. R.; Bueno, C.; Rheingold, A. L. *J. Am. Chem. Soc.* **1982**, *104*, 7347–7349.

(5) (a) Sappa, E.; Tiripicchio, A.; Braunstein, P. *Chem. Rev.* **1983**, *83*, 203–239. (b) Raithby, P. R.; Rosales, M. J. *Adv. Inorg. Chem. Radiochem.* **1985**, *29*, 170–247. (c) Nast, R. *Coord. Chem. Rev.* **1982**, *47*, 89–124.

(6) Silvestre, J.; Hoffmann, R. *Langmuir* **1985**, *1*, 621–647.

(7) Curtis, M. D.; Hay, M. S. *Inorg. Synth.* **1990**, *28*, 150–154.

(8) (a) Klinger, R. J.; Butler, W.; Curtis, M. D. *J. Am. Chem. Soc.* **1975**, *98*, 4645–4546. (b) Curtis, M. D. *Polyhedron* **1987**, *6*, 759–782. (c) Winter, M. J. *Adv. Organomet. Chem.* **1989**, *29*, 101–162.

(9) Baily, W. I., Jr.; Chisholm, M. H.; Cotton, F. A.; Rankel, L. A. *J. Am. Chem. Soc.* **1978**, *100*, 5764–5773.

(10) Bruce, M. I. *Chem. Rev.* **1991**, *91*, 197–257.

Table I. ^{13}C NMR Data for (CP)$_2$Mo$_2$(CO)$_4$(μ-FP—C≡C—H) (3)[a]

			chem shift					
complex[b]	temp, °C	solvent	*C*≡C—H	C≡*C*—H	Fe—CO	(CP)Fe	Mo—CO	(CP)Mo
3a (Fp–Cp)	27	CDCl$_3$	[c]	[c]	216.0	87.3	235.4	92.3
	–80	CD$_2$Cl$_2$	60.8 (d, 10.3)	110.0 (d, 212.6)	216.4, 216.6	87.7 (d, 181.7)	227.0, 230.1, 236.7, 239.2	91.7 (d, 175.9) 93.4 (d, 178.3)
3c (Fp*–Cp′)	27	C$_6$D$_6$	[c]	[c]	217.5	9.6, 95.7	235	14.3, 93
	–80	CD$_2$Cl$_2$	[c]	103.9 (d, 209)	216.1, 216.8	9.5 (d, 127.7) 89.4	229.0, 237.2,[d] 242.1	14.0 (q, 127.7) 86–96[e,f]
3d (Fp′–Cp)	27	CDCl$_3$	[c,g]	108.1[g]	215.8	13.2, 86.0, 88.3[h]	235.0	91.9 101.5[h]
	–80	CD$_2$Cl$_2$	61.4 (d, 10.9)	110.3 (d, 212.5)	216.8, 217.1	13.6 (q, 129), 85.7,[e] 87.7,[e] 88.8,[e] 89.2,[e] 102.3[h]	230.9, 236.31, 236.35, 239.1	91.6 (d, 176.1), 93.4 (d, 177.4)
3e (Fp^{Si}–Cp)	50[j]	C$_6$D$_6$	65.3[i]	107.2 (d, 208.4)	216.4	–0.8 (q, 119.7), 87.3,[h] 91.8 (d, 177.4), 95.1 (d, 178.8)	235.1	92.1 (d, 176.1)
	27	CDCl$_3$	66.4[i]	107.7 (d, 208)	215.8	–0.6 (q, 119.7), 87.2,[h] 91.3 (d, 177.5), 94.8 (d, 178.8)	234.8	91.9 (d, 176.1)
	–80	CD$_2$Cl$_2$	60.2 (d, 11.9)	110.2 (d, 212.3)	216.6, 217.1	–0.6 (q, 120.5), 84.2,[h] 92.0,[f] 92.7,[f] 94.9,[f] 96.5 (d, 180.0)	230.2, 236.0, 236.8, 239.1	91.8 (d, 177.2) 93.3 (d, 178.6)
4a[k] (H–Cp)	35	C$_6$D$_6$	61.9 (d, 216)				230.2	90.8 (d, 178)
	–90	[l]	[l]	[l]			229.2, 232.6	[l]
4b[k] (Ph–Cp)	room temp	[l]	[l]	[l]			229.9, 231.3	91.8
	–100	tol-d_8	[l]	[l]			227.8, 231.5, 232.4, 233.1	90.8, 92.5

[a] Observed at 68 MHz. δ, referenced to TMS, is reported in ppm, and multiplicities and coupling constants (*J*, Hz) are indicated in parentheses. The multiplicity of the signals is singlet unless otherwise stated, when the coupling constants are determined. A sample of **3b** of high enough concentration cannot be obtained. [b] The FP and CP parts are indicated in parentheses. [c] Cannot be located. [d] 2 CO's. [e] All the C$_5$H$_4$Me signals appear separately. [f] Doublet signals. The coupling constants cannot be determined owing to overlapping with other signals. [g] Broad signal. [h] The ipso carbons of the Cp′ and Cp^{Si} rings. [i] $^2J_{CH}$ cannot be determined. [j] δ's are calibrated by the solvent signal (C$_6$D$_6$: 128 ppm). [k] Reference 9. [l] Not reported.

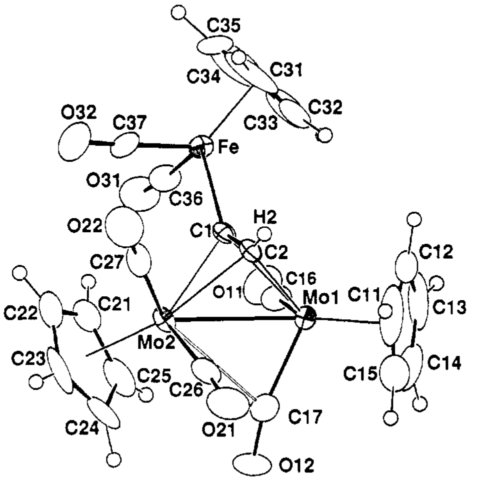

Figure 1. Molecular structure of **3a** drawn at the 30% probability level.

from an inductive effect of the FP group. δ_C(C≡C)'s of normal alkyne adducts fall in the range of 30–140 (usually 60–90), and in the case of unsymmetrical alkyne adducts the carbon atom attached to an electron-donating substituent is more shielded than the other carbon atom (for example, the H—C≡C—SiMe$_2$Ph adduct: δ_C(C—H) 100.7; δ_C(C—Si) 29.3).[11] Thus, the distortion of the C$_2$-Mo$_2$ core of **3a,e** may not be attributed to **B** but to the steric repulsion between the FP group and the ancillary ligands on Mo. Finally, the semibridging CO ligand is found in the Mo1–C17–O12 moiety.

Fluxional Behavior of (CP)$_2$Mo$_2$(CO)$_4$(μ-FP—C≡C—H)(3). **3a** turned out to be fluxional, as described above. However, we could not get a spectrum at the fast-exchange limit. Heating a benzene-d_6 solution of **3a** above 70 °C induced decomposition.

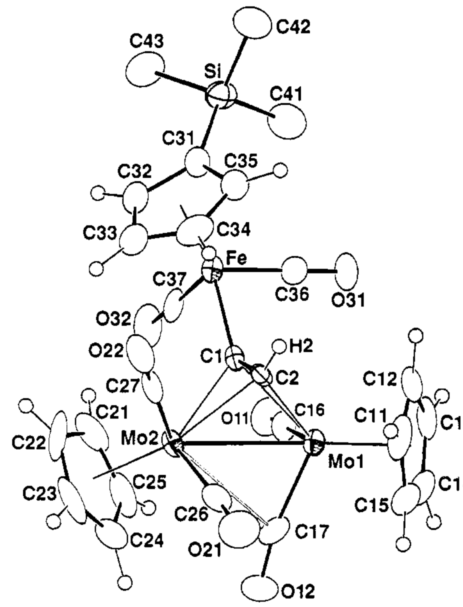

Figure 2. Molecular structure of **3e** drawn at the 30% probability level.

In order to get a fast-exchange-limit spectrum, we prepared and examined the adduct series **3b–e** bearing substituted Cp ligands (eq 2 and Table I). Af first we examined the Fp* analogue **3b**. Unfortunately, its poor solubility prevented us from getting a good ^{13}C NMR spectrum. Then Cp′ was introduced to the Mo$_2$ parts to increase the solubility (**3c**). While the solubility problem was solved, this complex also did not provide us with a fast-exchange-limit spectrum. Next, the Fp′ derivative of **3a** (**3e**) showed an indication of giving a fast-exchange-limit spectrum, but the C$_2$H signals were still considerably broad. Finally, we succeeded in getting both the fast- and slow-exchange-limit spectra of **3e**, bearing a bulky SiMe$_3$ substituent at the Fp moiety (Figure 3). At –80 °C, the

---

[11] Beck, J. A.; Knox, S. A. R.; Stansfield, R. F. D.; Stone, F. G. A.; Winter, M.; Woodward, P. *J. Chem. Soc., Dalton Trans.* **1982**, 195–200.

Table II. Crystallographic Data for 3a,e and 5a

	3a	3e	5a
formula	$C_{23}H_{16}O_6FeMo_2$	$C_{26}H_{24}O_6SiFeMo_2$	$C_{22}H_{16}O_5FeMo_2$
fw	636.1	708.3	608.1
space group	$P2_1/a$	$P2_1/c$	$P2_1/a$
a/Å	18.318(2)	12.608(3)	15.197(3)
b/Å	9.709(2)	23.224(12)	17.362(5)
c/Å	12.608(3)	9.172(2)	8.080(3)
β/deg	98.85(1)	96.11(2)	101.32(2)
V/Å^3	2216(1)	2670(3)	2090(1)
Z	4	4	4
d_{calcd}/g·cm^{-3}	1.90	1.76	1.93
μ/cm^{-1}	17.7	15.4	18.7
temp/°C	25	25	25
2θ/deg	2–55	2–50	2–55
no. of data collected	5595	5149	5320
no of data with $I > 3\sigma(I)$	3442	3967	2941
no. of variables	293	329	318
R	0.0444	0.0514	0.0464
R_w	0.0400	0.0558	0.0387

Table III. Comparison of Selected Structural Parameters for $Cp_2Mo_2(CO)_4(\mu\text{-}\eta^2\text{:}\eta^2\text{-}R{-}C{\equiv}C{-}H)$

	R = Fp (**3a**)	R = Fp^{Si} (**3e**)	R = H	Co complex[a]
	Bond Lengths (Å)			
C1–C2	1.321(9)	1.32(1)	1.337(5)	1.305(5)
C1–Fe	1.971(7)	1.994(8)		1.954(3)
C1–Mo1	2.330(7)	2.302(8)	2.203(3)	2.046(2)
C1–Mo2	2.294(7)	2.290(8)	2.172(3)	2.054(3)
C2–Mo1	2.113(8)	2.119(8)	2.122(3)	1.943(3)
C2–Mo2	2.205(7)	2.224(8)	2.190(3)	1.947(3)
C2–H2	0.71(5)	1.07(7)	0.98(6), 0.93(6)	1.09(4)
Mo1–Mo2	2.972(1)	2.984(1)	2.980(1)	
Mo1–C16	1.952(8)	1.938(9)	1.953(4)	
Mo1–C17	1.977(9)	1.92(1)	1.951(4)	
Mo2–C17	2.904(8)	2.926(9)	*b*	
Mo2–C26	1.975(8)	1.98(1)	1.989(3)	
Mo2–C27	1.955(9)	1.94(1)	1.993(4)	
	Bond Angles (deg)			
∠Fe–C1–C2	134.7(5)	132.6(6)	138(3), 139(3)[c]	146.9(2)
∠Mo1–C17–O12[d]	168.7(8)	169.9(8)	168.5(4)	

[a] $Co_2(CO)_6(\mu\text{-}\eta^2\text{:}\eta^2\text{-}Fp{-}C{\equiv}C{-}H)$.[1d] [b] Not available. [c] ∠H–C–C. [d] Semibridging CO.

Chart I

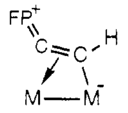

B

two CpMo ligands and all the carbon atoms of the C_2H, Fe—CO, Mo—CO, and $C_5H_4SiMe_3$ parts are observed separately. The Fe—CO signals and the CP and Mo—CO signals coalesce around −40 and −20 °C, respectively, and between −20 and 0 °C the C_2H signals become very broad. Further heating at 50 °C gives the fast-exchange-limit spectrum containing the two sharp C_2H signals and the single CpMo and Fe— and Mo—CO signals.

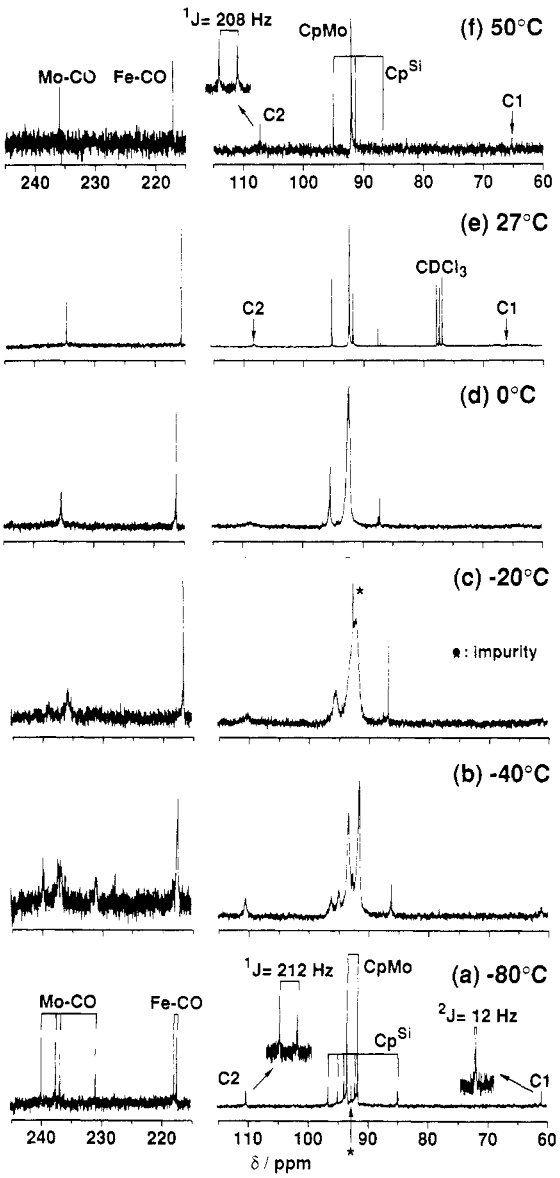

Figure 3. Variable-temperature ^{13}C NMR spectra of **3e** (the $SiMe_3$ region is omitted): (a) at −80 °C in CD_2Cl_2; (b) at −40 °C in CD_2Cl_2; (c) at −20 °C in CD_2Cl_2; (d) at 0 °C in CD_2Cl_2; (e) at 27 °C in $CDCl_3$; (f) at 50 °C in C_6D_6. For (a) and (f) the nondecoupled spectra are shown in insets.

Scheme I

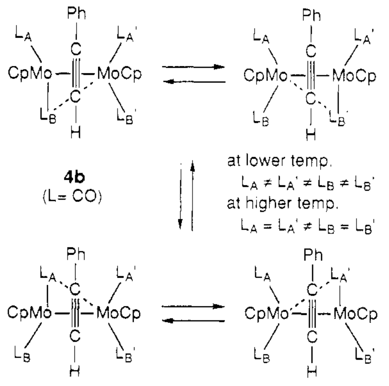

Two notable features can be deduced from the present VT ^{13}C NMR analyses: (1) The C_2H signals broaden in the medium-temperature range and appear as two doublets at the slow and fast exchange limit. (2) All the Mo—CO's are observed equivalently at higher temperature. In connection with the latter feature, Cotton et al. reported VT ^{13}C NMR of the Ph—C≡C—H adduct **4b**.[9] The four CO ligands observed inequivalently at low temperature appeared as two signals even at 90 °C (Table I). This spectral change has been explained consistently in terms of the switching process of the CO ligands as shown in Scheme I.

For an explanation of the first feature we propose a mechanism via the vinylidene intermediate **C** (Scheme

Scheme II

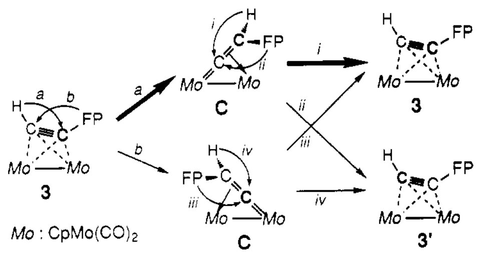

II), which is suggested by the following two reports and the structure of the photodecarbonylation product **5** (see the next section). Knox reported that irradiation of Cp*$_2$Mo$_2$(CO)$_4$ under a stream of ethyne afforded the μ-η^1:η^2-ethenylidene complex, which converted slowly to the μ-η^2:η^2-ethyne complex (eq 3).[12] Green also observed gradual thermal transformation of the dimolybdenum μ-η^1:η^2-vinylidene complexes to the μ-η^2:η^2-alkyne complexes

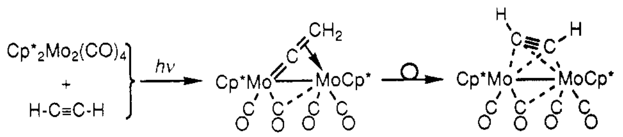

(3)

(eq 4).[13] **C** can be formed by way of H or FP migration,

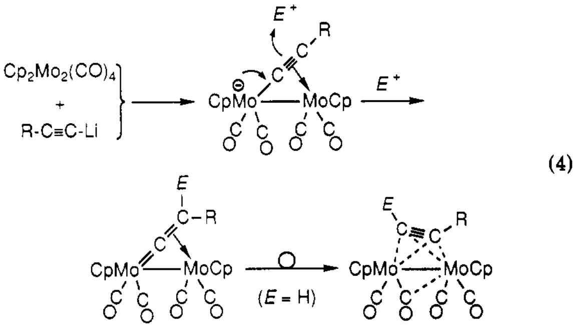

(4)

and the four migration types shown in Scheme II are possible depending on the combination of the mode of the migrations. These pathways may be discriminated partly by examining the spectral change of the C$_2$H part. If the reversible migration (a-i or b-iii in Scheme II) occurs, warming the sample brings about broadening of the two C$_2$H signals in the medium-temperature range and finally they appear as two sharp doublets. On the other hand, if the other H—FP exchange mechanism (a-ii or b-iv) operates, the C$_2$H carbon atoms, observed separately at low temperature, coalesce and, at the fast-exchange limit, should be observed as a doublet whose δ_C and J_{CH} values are equal to the averaged values of the corresponding parameters of C$_\alpha$ and C$_\beta$ at the slow-exchange limit.[14] Actually, **3** follows the reversible process (a-i or b-iii), as is evident from the spectra shown in Figure 3. Although we cannot exclude the possibility of FP migration (b-iii), the shift of the hydrogen atom with the spherical 1s orbital (a-i) is apparently preferable over that of the FP group (b-iii). The 1,2-H migration on the Cp$_2$Mo$_2$(CO)$_4$(μ-R— and FP—C≡C—H) system may proceed in a way similar to the 1-alkyne-to-vinylidene ligand transformation within a mononuclear transition-metal coordination sphere.[10,15,16] In any event, it should be noted that the FP groups remarkably labilize the hydrogen atom at C$_\beta$ in **3**.

The Mo—CO scrambling (feature 2) cannot be explained even by taking account of the 1,2-H migration mechanism. Possible mechanisms include (a) exchange of an Mo—CO ligand with the other CO attached to the same Mo atom, (b) rotation of the FP—C≡C—H part, (c) nonstereospecific 1,2-H migration, (d) rotation of the μ-η^1:η^2-vinylidene ligand in **C** while maintaining interaction with the two Mo centers, and (e) rotation via an η^1- or μ-vinylidene intermediate. Although (a) and (b) may be eliminated on the basis of Cotton's experiment, where such a process was not observed for **4b** even at 90 °C,[9] we have no NMR evidence to discriminate the remaining mechanisms. The fluxional process of the μ-η^1:η^2-vinylidene complexes shown in eq 4 has been interpreted in terms of intermediates such as those appearing in (d) and (e).[13] Furthermore, the CO scrambling may be connected to the above-mentioned dynamic process of the FP—C≡C—H part.

Photochemical Decarbonylation of 3 Leading to the μ_3-Vinylidenyl Complexes 5. Irradiation of a benzene or toluene solution of **3a,b** by a high-pressure mercury lamp exclusively afforded an isomeric mixture of the decarbonylated product **5a,b** in moderate yields, respectively (eq 5), and the decarbonylation proceeded slowly even in daylight. The composition of the isomers was determined to be 1.6:1 (**5a**) and 4.5:1 (**5b**) by means of ^{1}H NMR.

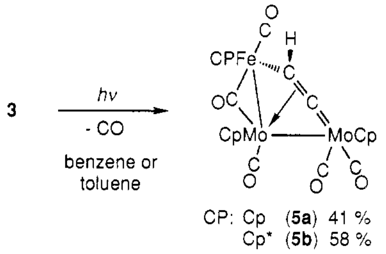

(5)

Although the NMR data for **5** shown in Chart II indicate the presence of a trinuclear μ_3-vinylidenyl (ethenylidenyl) structure, the arrangement of the metal atoms cannot be determined by the spectral data alone. Therefore, the molecular structure of **5a** was confirmed by X-ray crystallography (Figure 4 and Table IV).

The μ_3-C$_2$H ligand coordinates to the FeMo$_2$ backbone in an η^1(Fe):η^2(Mo1):η^1(Mo2) fashion, and the structure of the Mo$_2$(μ-C$_2$H) part is close to the core structure of **6** (Chart III),[13] which is best described as a μ-η^1:η^2-vinylidene complex. Thus, **5a** is viewed as an analogue of **6** bearing the Fe group as a vinylidene substituent. In addition, the structure of **5a** strongly supports the intermediacy of **C** during the above-mentioned fluxional behavior of **3**.

---

[12] Doherty, N. M.; Elschenbroich, C.; Kneuper, H.-J.; Knox, S. A. R. *J. Chem. Soc., Chem. Commun.* **1985**, 170–171. For the structure of the Cp analogue of the ethenylidene complex, see: Kern, U.; Kreiter, C. G.; Muller-Becker, S.; Frank, W. *J. Organomet. Chem.* **1993**, *444*, C31–33.

[13] Froom, S. F. T.; Green, M.; Mercer, R. J.; Nagle, K. R.; Orpen, A. G.; Rodriques, R. A. *J. Chem. Soc., Dalton Trans.* **1991**, 3171–3183.

[14] A similar spectral change was observed for the cationic μ-ethynyl complex [Fp*$_2$(μ-C$_2$H)]BF$_4$, though the mechanism was different.[1a]

[15] Silvestre, J.; Hoffmann, R. *Helv. Chim. Acta* **1985**, *68*, 1461–1506.

[16] An H migration to the metal framework affording a hydrido–acetylido intermediate was suggested by one of the reviewers. Although a subsequent 1,3-H shift giving the vinylidene ligand is an unfavorable process for a mononuclear system,[15] such a reaction mechanism may be possible for a dinuclear system.

[17] Although **5** with a C$_2$H ligand may be viewed as an acetylide cluster compound, as suggested by a reviewer, the similarity of the structural characteristics with those of **6** clearly indicate that **5** is best described as a vinylidene complex. To our knowledge, an acetylide cluster compound containing a linear M–C–C linkage such as **5** has not been reported (usually <160°).

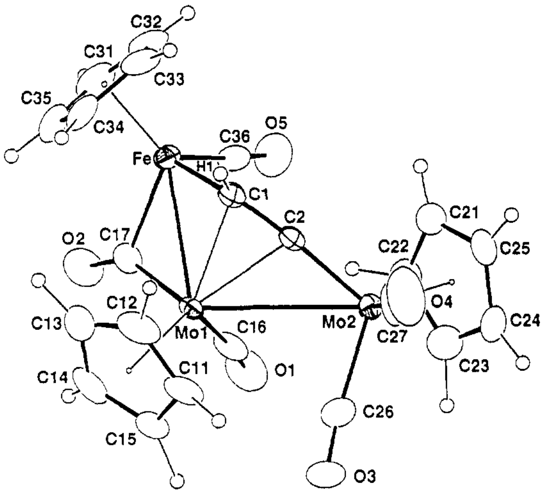

Figure 4. Molecular structure of **5a** drawn at the 30% probability level.

Chart II

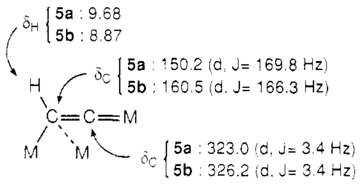

Table IV. Selected Interatomic Distances (Å) and Bond Angles (deg) for 5a

	Interatomic Distances[a]		
C1-C2	1.338(9)	Mo2-C26	1.998(9)
-H1	0.97(7)	-C27	1.920(8)
-Fe	1.929(7)	-(C21-25)	2.353
-Mo1	2.242(6)	-CP2	2.028
C2-Mo1	2.208(5)	Fe-C17	2.063(7)
-Mo2	1.901(6)	-C36	1.743(6)
Mo1-Mo2	3.172(1)	-(C31-35)	2.100
-Fe	2.799(1)	-CP3	1.704
Mo1-C16	1.974(7)	C16-O16	1.146(8)
-C17	2.024(7)	C17-O17	1.196(9)
Mo1-(C11-15)	2.342	C26-O26	1.138(10)
-CP1	2.014	C27-O27	1.176(11)
Mo2-Fe	4.528(1)	C36-O36	1.138(8)
	Bond Angles		
C2-C1-H1	123(4)	C1-Mo1-C2	35.0(2)
-Fe	123.7(5)	-Fe	43.3(2)
-Mo1	71.1(4)	-Mo2	71.0(2)
Fe-C1-H1	113(4)	C2-Mo1-Fe	69.5(2)
-Mo1	83.9(2)	-Mo2	36.1(2)
H1-C1-Mo1	124(4)	-Mo1	43.1(2)
C1-C2-Mo1	73.9(4)	Mo2-Mo1-Fe	98.43(2)
-Mo2	173.5(5)	C1-Fe-Mo1	52.8(2)
Mo1-C2-Mo2	100.8(3)		

[a] Bond lengths without standard deviations are averaged lengths.

Chart III

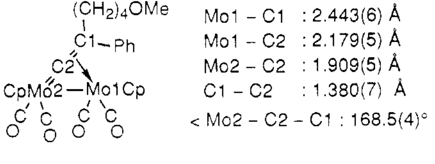

Chart IV

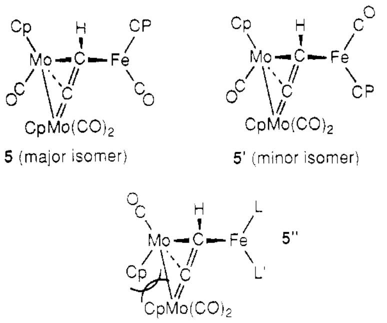

Scheme III

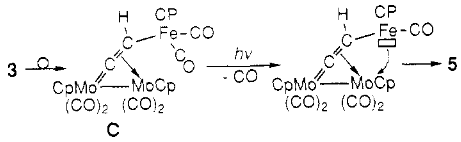

Scheme IV

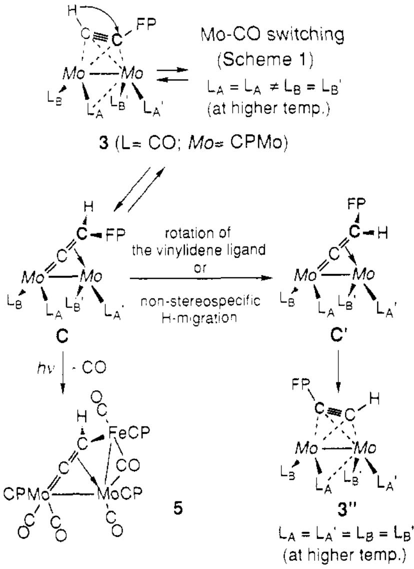

The NMR spectra of the reaction mixtures indicate the formation of two isomers, which may arise from the stereoisomerism with respect to the sterically congested FeMo1 core. In the X-ray structure of **5a**, the Cp ligands attached to Fe and Mo1 occupy the opposite side of the Mo2 part. Because the other orientation of the Mo1—Cp and —CO ligands (**5''**) apparently induces steric repulsion, we have tentatively assigned the two isomers to **5** (the major isomer) and **5'** (the minor isomer) (Chart IV).

Formation of **5a,b** may be initiated by the isomerization of **3** to the vinylidene form **C** (Scheme III). Successive decarbonylation from the Fp part and electrophilic attack at the π-coordinated Mo center may lead to **5a,b**. The coordinative unsaturation generated by the photochemical decarbonylation is compensated by the formation of the Fe—Mo bond with the bridging CO.

Conclusion

The ethynyliron complexes FP—C≡C—H (**1**) readily react with (CP)$_2$Mo$_2$(CO)$_4$ (**2**) to give the adducts (CP)$_2$Mo$_2$(CO)$_4$(μ-η^2:η^2-FP—C≡C—H) (**3**) with a tetrahedral C$_2$Mo$_2$ core and semibridging CO ligand. The core structures of **3a,e** are found to be close to those of normal alkyne adducts. In contrast to the previously studied Co$_2$(CO)$_8$ and Cp$_2$Ni$_2$(CO)$_2$ adducts of **1a,b**, a remarkable H labilization is brought about by the FP group in the Mo$_2$ adducts **3**. The whole fluxional process of **3** is summarized in Scheme IV. In addition to the CO switching process which has been generally observed for normal alkyne adducts, the H atom migrates between C$_\beta$ and C$_\alpha$

Scheme V

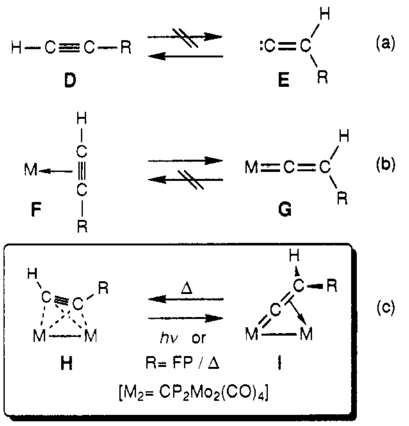

via **C** at a rate comparable to or faster than the NMR time scale above room temperature. Moreover, all the Mo—CO's are observed equivalently at higher tmeperature via an undertermined mechanism.

Although 1-alkyne-to-vinylidene tautomerization (**D** → **E**) is recognized as a highly unfavorable process owing to the thermodynamic instability of the vinylidene species **E** ((a) in Scheme V),[18] coordination to a transition metal results in inversion of the energetics (b). The inversion originates from availability of a π^* orbital of suitable symmetry which receives d electrons effectively through back-donation, as clearly indicated in the EHMO analysis by Hoffmann et al.[15] A number of η^1-vinylidene complexes (**G**) have been prepared by this route,[10] and an increasing number of catalytic reactions involving this isomerization as a key step have been reported.[19] In contrast to paths a and b, little information on dinuclear systems (c) has been accumulated so far. To our knowledge, reports on the **I**-type structure have been limited to the Cp$_2$Mo$_2$(CO)$_4$ system.[10,11,12,13,20] As shown in eqs 3 and 4, the backward transformation (**I** → **H**) proceeded slowly at the dimolybdenum center. On the other hand, little evidence for the forward process has appeared except for Knox's photochemical experiment, which suggests the intermediacy of **H** before formation of **I**. The present study indicates that, if the thermodynamic stabilities of **H** and **I** are balanced, the 1-alkyne-to-vinylidene ligand transformation (**H** → **I**) is possible on a dinuclear system under thermal conditions.[21,22]

Finally, irradiation of **3** results in decarbonylation to give the μ_3-vinylidenyl complex **5**, which supports **C** (**I**).

Experimental Section

General Considerations. All manipulations were carried out under an argon atmosphere by using standard Schlenk-tube techniques. Ether, hexanes, benzene, and toluene (Na-K alloy/benzophenone) and CH$_2$Cl$_2$ (P$_2$O$_5$) were treated with appropriate drying agents, distilled, and stored under Ar. **1a**,[2b] **1b**,[1a] Cp$_2$Mo$_2$(CO)$_6$,[23] **2a**,[7] and Cp'$_2$Mo$_2$(CO)$_6$[23] were prepared according to the literature procedures. **1c**,**d** were prepared by the reaction of the corresponding FP—I[24] with H—C≡C—MgBr in a manner similar to that for **1a**. Cp$_2$W$_2$(CO)$_6$ and alumina were purchased from Aldrich and Merck (activity II-IV: Art. 1097), respectively, and used as received.

^{1}H and ^{13}C NMR spectra were recorded on JEOL EX-90 and JEOL GX-270 spectrometers, respectively (^{1}H, 90 MHz; ^{13}C, 67.9 MHz). IR and FD-MS spectra were obtained on a JASCO FT/IR-5300 spectrometer and a Hitachi M-80 mass spectrometer, respectively.

Preparation of Cp$_2$Mo$_2$(CO)$_4$(μ-η^2:η^2-Fp—C≡C—H) (3a). A benzene solution (30 mL) of Cp$_2$Mo$_2$(CO)$_6$ (557 mg, 1.14 mmol) was refluxed for 9 h with maintenance of a slow Ar bubbling.[7] To the resulting solution cooled to room temperature was added **1a** (260 mg, 1.29 mmol), and the mixture was stirred overnight. After evaporation of the volatiles the product was extracted with ether and filtered through an alumina pad. Crystallization from ether–hexanes gave **3a** as deep purple-red crystals (335 mg, 0.53 mmol, 46% yield). ^{1}H NMR (CDCl$_3$, at 27 °C): δ 6.76 (s, 1H, C$_2$*H*), 5.30 (s, 10H, 2CpMo), 4.85 (s, 5H, CpFe). IR (KBr): 2011, 1953, 1885, 1870, 1819, 1810 cm^{-1}. Anal. Calcd for C$_{23}$H$_{16}$O$_6$FeMo$_2$: C, 43.43; H, 2.54. Found: C, 43.32; H, 2.58. FDMS: *m/e* 636 (M$^+$).

Preparation of Cp$_2$Mo$_2$(CO)$_4$(μ-η^2:η^2-Fp*—C≡C—H) (3b). A benzene solution (20 mL) of **1b** (215 mg, 0.790 mmol) and **2a** (295 mg, 0.680 mmol) was stirred for 5 h at room temperature. The supernatant was removed via a pipet, and the remaining solid was washed with hexanes (5 mL × 5). After it was dried in vacuo, **3b** was isolated as a purple-red solid in 82% yield (393 mg, 0.556 mmol). An analytically pure sample could not be obtained. ^{1}H NMR (CDCl$_3$, at 27 °C): δ 7.06 (s, 1H, C$_2$*H*), 5.17 (s, 10H, 2CpMo), 1.71 (s, 15H, Cp*Fe). IR (KBr): 1997, 1950, 1931, 1871, 1861, 1803 cm^{-1}. FDMS: *m/e* 706 (M$^+$).

Preparation of Cp'$_2$Mo$_2$(CO)$_4$(μ-η^2:η^2-Fp*—C≡C—H) (3c). A toluene solution (20 mL) of Cp'$_2$Mo$_2$(CO)$_6$ (1.00 g, 1.93 mmol) was refluxed for 6 h with maintenance of a slow Ar bubbling. To the resulting mixture cooled to room temperature was added **1b** (520 mg, 1.91 mmol). After the mixture was stirred overnight, the volatiles were removed under reduced pressure. Extraction with CH$_2$Cl$_2$ and filtration through a Celite pad followed by crystallization from CH$_2$Cl$_2$–hexanes gave brown-black **3c** (920 mg, 1.25 mmol, 66% yield). ^{1}H NMR (CDCl$_3$, at 27 °C): δ 6.64 (s, 1H, C$_2$*H*), 5.0–5.2 (m, 4H, C$_5$*H*$_4$Me), 2.10 (3H, br s, C$_5$H$_4$*Me*), 1.78 (s, 15H, Cp*Fe). IR (KBr): 1993, 1952, 1862, 1799 cm^{-1}. Anal. Calcd for C$_{30}$H$_{30}$O$_6$FeMo$_2$: C, 49.07; H, 4.12. Found: C, 49.00; H, 4.11.

Preparation of Cp$_2$Mo$_2$(CO)$_4$(μ-η^2:η^2-Fp'—C≡C—H) (3d). A toluene solution (20 mL) of **1c** (323 mg, 1.50 mmol) and Cp$_2$Mo$_2$(CO)$_4$ (466 mg, 1.07 mmol) was stirred overnight at room temperature. After evaporation of the volatiles the products were extracted with ether and passed through an alumina pad. Purple-brown **3d** (355 mg, 0.55 mmol, 51% yield) was crystallized from ether–hexanes. ^{1}H NMR (CDCl$_3$, at 27 °C): δ 6.981 (s, 1H, C$_2$*H*), 5.31 (s, 10H, 2CpMo), 4.53 (m, 2H, C$_5$*H*$_4$Me), 4.77 (m, 2H, C$_5$*H*$_4$Me), 2.00 (br s, 3H, C$_5$H$_4$*Me*). IR (KBr): 2002, 1962, 1951, 1899, 1854, 1794 cm^{-1}. Anal. Calcd for C$_{24}$H$_{18}$O$_6$FeMo$_2$: C, 44.34; H, 2.79. Found: C, 44.08; H, 2.87.

Preparation of Cp$_2$Mo$_2$(CO)$_4$(μ-η^2:η^2-Fp^{Si}—C≡C—H) (3e). A toluene solution (20 mL) of Cp$_2$Mo$_2$(CO)$_6$ (1.00 g, 2.04 mmol) was refluxed for 6 h with maintenance of a slow Ar bubbling. To the resulting mixture cooled to room temperature was added **1d** (650 mg, 2.37 mmol). After the mixture was stirred overnight, the volatiles were removed under reduced pressure. Extraction with CH$_2$Cl$_2$ and filtration through an alumina pad followed by crystallization from hexanes gave dark brown **3e** (691 mg, 0.98

---

[18] See references cited in ref 10.

[19] (a) Wakatsuki, Y.; Yamazaki, H.; Kumegawa, N.; Satoh, T.; Satoh, J. Y. *J. Am. Chem. Soc.* **1991**, *113*, 9604–9610. (b) Trost, B. M.; Kulawiec, R. J. *J. Am. Chem. Soc.* **1992**, *114*, 5579–5584. (c) See also references cited in ref 10.

[20] Rh$_2$ complexes without a metal–metal bond were reported. Werner, H.; Wolf, J.; Muller, G.; Kruger, C. *Angew. Chem., Int. Ed. Engl.* **1984**, *23*, 431–432. Werner, H.; Wolf, J.; Muller, G.; Kruger, C. *J. Organomet. Chem.* **1988**, *342*, 381–398.

[21] Any indication of the H migration was not detected at all for the Co$_2$ and Ni$_2$ adducts of **1a**,**b**.[1d,e]

[22] Very recently, 1-alkyne-to-vinylidene transformation on a planar dinuclear system was reported. Xiao, J.; Cowie, M. *Organometallics* **1993**, *12*, 463–472.

[23] (a) Manning, A. R.; Hackett, P.; Birdwhistell, R.; Soye, P. *J. Organomet. Chem.* **1978**, *157*, 239–241. (b) Birdwhistell, R.; Hackett, P.; Manning, A. R. *Inorg. Synth.* **1990**, *28*, 150–154.

[24] Fp^{Si}—I was prepared by I$_2$ treatment of LiFp^{Si}, which was generated by the reaction of Fp—SiMe$_3$ with *n*-BuLi: Berryhill, S. R.; Clevenger, G. L.; Burdurlu, F. Y. *Organometallics* **1985**, *4*, 1509–1515. King, R. B.; Pannell, K. H. *Inorg. Chem.* **1968**, *7*, 1510–1513.

mmol, 48% yield). ^{1}H NMR (CDCl$_3$, at 27 °C): δ 6.76 (s, 1H, C$_2$*H*), 5.31 (s, 10H, 2CpMo), 4.9 (m, 4H, C$_5$*H*$_4$SiMe$_3$), 0.25 (s, 9H, SiMe$_3$). IR (KBr): 2018, 1976, 1949, 1894, 1873, 1861, 1823 cm^{-1}. Anal. Calcd for $C_{26}H_{24}O_6SiFeMo_2$: C, 44.09; H, 3.42. Found: C, 43.99; H, 3.50.

Photodecarbonylation of 3a Giving 5a. A toluene solution (70 mL) of **3a** (1.02 g, 1.60 mmol) in a quartz Schlenk tube was irradiated by a high-pressure mercury lamp for 2 h. After evaporation of the volatiles the residue was washed with hexanes, extracted with CH$_2$Cl$_2$, and filtered through an alumina pad. Crystallization from CH$_2$Cl$_2$–hexanes gave **5a** as green-black crystals (340 mg, 0.56 mmol). From the mother liquor more **5a** (61 mg, 0.10 mmol) was obtained: total yield 41%. IR (KBr): 1958, 1930, 1885, 1837, 1735 cm^{-1}. Anal. Calcd for $C_{22}H_{16}O_5FeMo_2$: C, 43.45; H, 2.65. Found: C, 43.55; H, 2.80. FDMS: *m/e* 608 (M$^+$). **5a** (major): ^{1}H NMR (CDCl$_3$) δ 9.68 (s, 1H, C$_2$H), 5.18, 5.37 (s × 2, 5H × 2, 2CpMo), 4.83 (s, 5H, FeCp); ^{13}C NMR (CDCl$_3$) δ 323.0 (d, *J* = 3.4 Hz, *C*=CH), 268.4 (s, μ-CO), 232.3, 231.6, 220.0, 215.1 (s × 4, 4CO), 150.2 (d, *J* = 169.8 Hz, C=*C*H), 95.1 (d, *J* = 178.3 Hz, CpMo), 93.5 (d, *J* = 176.6 Hz, CpMo), 85.2 (d, *J* = 178.3 Hz, CpFe). **5a′** (minor): ^{1}H NMR (CDCl$_3$) δ 8.19 (s, 1H, C$_2$H), 5.12, 5.51 (s × 2, 5H × 2, 2CpMo), 4.46 (s, 5H, FeCp); ^{13}C NMR (CDCl$_3$) δ 316.8 (br, *C*=CH), 276.0 (s, μ-CO), 234.5, 232.5, 220.1, 213.9 (s × 4, 4CO), 142.7 (d, *J* = 178.3 Hz, C=*C*H), 96.3 (d, *J* = 183.5 Hz, CpMo), 94.2 (d, *J* = 176.5 Hz, CpMo), 86.3 (d, *J* = 178.3 Hz, CpFe).

Photodecarbonylation of 3b Giving 5b. A benzene solution (40 mL) of **3b** (360 mg, 0.51 mmol) in a quartz Schlenk tube was irradiated by a high-pressure mercury lamp for 3 h. Workup as described above and crystallization from CH$_2$Cl$_2$–hexanes gave **5b** as green-black microcrystals (230 mg, 0.30 mmol, 58%). IR (KBr): 1940, 1916, 1861, 1721 cm^{-1}. Anal. Calcd for $C_{27}H_{26}O_5FeMo_2$: C, 47.82; H, 3.86. Found: C, 47.95; H, 4.01. FDMS: *m/e* 678 (M$^+$). **5b** (major): ^{1}H NMR (CDCl$_3$) δ 8.87 (s, 1H, C$_2$H), 5.18, 5.36 (s × 2, 5H × 2, 2CpMo), 1.83 (s, 15H, FeCp*); ^{13}C NMR (CDCl$_3$) δ 326.2 (d, *J* = 3.4 Hz, *C*=CH), 274.9 (s, μ-CO), 234.2, 234.0, 220.7, 215.6 (s × 4, 4CO), 160.5 (d, *J* = 166.3 Hz, C=*C*H), 96.3 (s, *C*$_5$Me$_5$), 94.2 (d, *J* = 177.0 Hz, CpMo), 93.2 (d, *J* = 177.0 Hz, CpMo), 9.9 (q, 127.2 Hz, C$_5$*Me*$_5$). **5b′** (minor): ^{1}H NMR (CDCl$_3$) δ 5.14, 5.29 (s × 2, 5H × 2, 2CpMo), 1.72 (s, 15H, FeCp*) (a small peak at δ 6.59 may be attributed to C$_2$H).

X-ray Crystallography of 3a,e and 5a. **3a** and **5a** were recrystallized from an ether–hexanes mixed-solvent system and **3e** from CH$_2$Cl$_2$–hexanes, and suitable crystals were mounted on glass fibers. Diffraction measurements were made on a Rigaku AFC-5 automated four-circle diffractometer by using graphite-monochromated Mo Kα radiation (λ = 0.710 59 Å). The unit cell was determined and refined by a least-squares method using 25 independent reflections. Data were collected with the ω–2θ scan technique. If $\sigma(F)/F$ was more than 0.1, a scan was repeated up to three times and the results were added to the first scan. Three standard reflections were monitored after every 100 measurements. All data processing was performed on an IRIS Indigo computer by using the TEXSAN structure-solving program system (**3a,e**) and on a FACOM A70 computer by using the R-CRYSTAN structure-solving system (**5a**) obtained from the Rigaku Corp., Tokyo, Japan. Neutral scattering factors were obtained from the standard source.[25] In the reduction of data, Lorentz and polarization corrections were made.

3a,e and **5a** crystallized in a monoclinic system. The structures were solved by a combination of direct methods and difference Fourier synthesis by using the TEXSAN (**3a,e**) and R-CRYSTAN (**5a**) structure-solving system. For **3a,e** all the non-hydrogen atoms were refined anisotropically, and the C$_2$*H* atoms located by Fourier synthesis were refined isotropically. Although during the refinement a couple of the Cp rings were found to be disordered, the minor components were not included. The positions of the hydrogen atoms attached to the Cp groups were fixed at the ideal positions (d_{C-H} = 0.95 Å) and were not refined (B(H) = 1.1[B(C)]). For **5a** all the non-hydrogen atoms were refined anisotropically. Positions of all the hydrogen atoms were confirmed with B(H) = B(C).

Acknowledgment. This study was supported in part by a grant from the Ministry of Education, Science, and Culture of the Japanese Government. Thanks are also due to Dr. Yoshiyuki Nakamura for measurements of the VT ^{13}C NMR spectra.

Supplementary Material Available: Tables of positional and anisotropic thermal parameters and bond lengths and angles for **3a,e** and **5a** (15 pages). Ordering information is given on any current masthead page.

OM930126N

---

[25] *International Tables for X-Ray Crystallography*; Kynoch Press: Birmingham, U.K., 1975; Vol. 4.